Impact of TROPICS Radiances on Tropical Cyclone Prediction in an OSSE

HUI W. CHRISTOPHERSEN,[a] BRITTANY A. DAHL,[b,c] JASON P. DUNION,[b,c] ROBERT F. ROGERS,[c] FRANK D. MARKS,[c] ROBERT ATLAS,[d] AND WILLIAM J. BLACKWELL[e]

[a] *Naval Research Laboratory, Monterey, California*
[b] *Cooperative Institute for Marine and Atmospheric Studies, University of Miami, Miami, Florida*
[c] *NOAA/Atlantic Oceanographic and Meteorological Laboratory/Hurricane Research Division, Miami, Florida*
[d] *NOAA/Atlantic Oceanographic and Meteorological Laboratory, Miami, Florida*
[e] *Lincoln Laboratory, Massachusetts Institute of Technology, Lexington, Massachusetts*

(Manuscript received 19 October 2020, in final form 19 February 2021)

ABSTRACT: As part of the NASA Earth Venture-Instrument program, the Time-Resolved Observations of Precipitation structure and storm Intensity with a Constellation of Smallsats (TROPICS) mission, to be launched in January 2022, will deliver unprecedented rapid-update microwave measurements over the tropics that can be used to observe the evolution of the precipitation and thermodynamic structure of tropical cyclones (TCs) at meso- and synoptic scales. TROPICS consists of six CubeSats, each hosting a passive microwave radiometer that provides radiance observations sensitive to atmospheric temperature, water vapor, precipitation, and precipitation-sized ice particles. In this study, the impact of TROPICS all-sky radiances on TC analyses and forecasts is explored through a regional mesoscale observing system simulation experiment (OSSE). The results indicate that the TROPICS all-sky radiances can have positive impacts on TC track and intensity forecasts, particularly when some hydrometeor state variables and other state variables of the data assimilation system that are relevant to cloudy radiance assimilation are updated. The largest impact on the model analyses is seen in the humidity fields, regardless of whether or not there are radiances assimilated from other satellites. TROPICS radiances demonstrate large impact on TC analyses and forecasts when other satellite radiances are absent. The assimilation of the all-sky TROPICS radiances without default radiances leads to a consistent improvement in the low- and midtropospheric temperature and wind forecasts throughout the 5-day forecasts, but only up to 36-h lead time in the humidity forecasts at all pressure levels. This study illustrates the potential benefits of TROPICS data assimilation for TC forecasts and provides a potentially streamlined pathway for transitioning TROPICS data from research to operations postlaunch.

SIGNIFICANCE STATEMENT: As the Global Observing System evolves, smaller satellites such as CubeSats are emerging as inexpensive alternatives for providing important observations of Earth as compared to traditional satellites. TROPICS, to be launched in January 2022, is one of the NASA CubeSats missions that will deliver unprecedented rapid-update microwave measurements over the tropics. This study examines the impacts of simulated radiances from the TROPICS constellation of satellites for tropical cyclone analyses and forecasts in a regional mesoscale model and demonstrates the potential benefits of TROPICS data assimilation on TC forecasts. The infrastructure to incorporate the new TROPICS datasets into the operational model that was developed for this study will facilitate a transition from research to operations once the TROPICS data becomes available after the mission launch.

KEYWORDS: Tropical cyclones; Remote sensing; Data assimilation; Ensembles

1. Introduction

The observing system simulation experiment (OSSE) has long been used as a framework to quantify the potential impacts of current or proposed observing systems on numerical weather prediction (NWP) analyses and forecasts (Arnold and Dey 1986; Hoffman and Atlas 2016). This framework can provide a quantitative assessment that can help agencies to make informed decisions about observing systems in a cost-effective manner. It can also be used to evaluate alternative data assimilation (DA) schemes to further improve NWP (Kleist and Ide 2015a,b). In an OSSE, observations are simulated from a nature run, which is a realistic model simulation that is treated as the truth and should therefore be rigorously validated to ensure physical realism (Reale et al. 2007; Nolan et al. 2013). The simulated observations are assimilated into a forecast model, and the resulting analyses and forecasts are then verified against the nature run to estimate the impacts of the observing system.

This study utilizes the OSSE approach to demonstrate the potential impact of assimilating satellite radiances from the Time-Resolved Observations of Precipitation structure and storm Intensity with a Constellation of Smallsats (TROPICS) mission on tropical cyclone (TC) analyses and forecasts in a regional model. As part of the NASA Earth Venture-Instrument program, TROPICS will provide unprecedented rapid-refresh microwave (MW) measurements over the tropics that can be used to observe the evolution of the precipitation and thermodynamic structure of TCs at the mesoscale and synoptic scales (Blackwell et al. 2018). The launch of the

Atlas: Retired.

Corresponding author: Hui Christophersen, hui.christophersen@nrlmry.navy.mil

DOI: 10.1175/MWR-D-20-0339.1

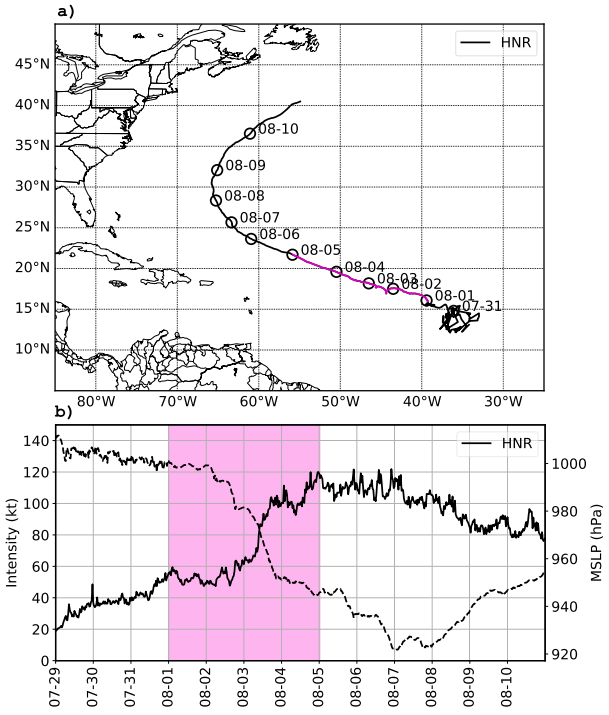

FIG. 1. HNR TC track, intensity (kt), and MSLP (hPa). The time period investigated in the OSSE is highlighted in magenta.

TROPICS satellites will be spaced out over a 6-month period beginning in January 2022 and ending in July 2022. TROPICS will consist of six identical MicroMAS-2 CubeSats evenly distributed in three low-Earth orbital planes. MicroMAS-2 is a 3U CubeSat with heritage from the MicroMAS-1 and Microwave Radiometer Technology Acceleration (MiRaTA) flight designs (Blackwell 2017). Each CubeSat hosts a passive MW radiometer providing atmospheric measurements sensitive to temperature, water vapor, precipitation, and cloud ice.

This study assimilates simulated TROPICS cloudy and precipitation-affected radiances in a regional mesoscale DA system to demonstrate the potential impact of the TROPICS data on TC prediction. In recent decades, many NWP centers have developed and implemented the assimilation of cloud- and precipitation-affected satellite radiances (also known as an ''all-sky'' approach) over land and ocean in their global DA systems (Geer et al. 2018). All-sky satellite radiance assimilation extracts information directly from the radiances regardless of whether they are obtained in clear, cloudy, or precipitating conditions. Some operational centers, such as the European Centre for Medium-Range Weather Forecasts (ECMWF), already routinely assimilate cloud- and precipitation-affected MW radiances in addition to clear-sky radiances, and by doing so have demonstrated significant improvements to model analyses and medium-range forecasts (Geer et al. 2018). In particular, there are promising results on improving analyses and forecasts of TC structure and intensity with the all-sky MW observations in the global system. For instance, the Japan Meteorological Agency (JMA) carried out all-sky MW assimilation in its global system with a four-dimensional variational (4DVAR) method and showed an improved representation of a TC undergoing rapid intensification (Geer et al. 2018).

In regional modeling systems, a few demonstration studies have shown that assimilating all-sky MW radiances results in positive impacts on TC predictions. Yang et al. (2016) evaluated the all-sky assimilation of the Advanced Microwave Scanning Radiometer 2 (AMSR2) within the Weather Research and Forecasting (WRF) Model's data assimilation (WRFDA) system using the three-dimensional variational (3DVAR) method. The results suggested that all-sky AMSR2 radiance assimilation consistently improved TC track and intensity forecasts and the overall representation of storm structure in the model. A similar study, evaluating the all-sky assimilation of the Microwave Humidity Sounder-2 (MWHS-2) radiances with the WRFDA-3DVAR, also demonstrated positive impacts on binary typhoon track and intensity forecasts and heavy rainfall prediction (Xian et al. 2019). Wu et al. (2019) assimilated all-sky radiances from the Advanced Technology Microwave Sounder (ATMS) with the Hurricane Weather Research and Forecasting (HWRF) Model using the hybrid Gridpoint Statistical Interpolation (GSI) analysis system and showed a better fit to observations and improved cloud signatures that were closer to observations. While Li et al. (2019) demonstrated great relative value of assimilating the MicroMAS-2 CubeSat observations into the numerical model, the approach to assimilating the satellite data in that study is nontraditional—using a linear regression method to convert the MicroMAS-2 radiances to the equivalent ATMS radiances. Direct assimilation of radiances is usually a preferred approach for operational transition (Bauer et al. 2006, 2010; Zhu et al. 2016); therefore, this study will directly assimilate TROPICS all-sky radiances to quantitatively assess their impacts on TC prediction.

The organization of this paper is as follows. A brief overview of the hurricane nature run and the characteristics of TROPICS satellite radiances and baseline control datasets are described in section 2. The forecast model, DA technique, and experimental design are addressed in section 3. Technical details of assimilating TROPICS radiances are discussed in section 4. The impact of using new state variables in the DA system is addressed in section 5. The TROPICS radiance impacts with and without the default radiances are presented in section 6, followed by a summary and concluding remarks.

2. Data description

a. Overview of the hurricane nature run

The Nolan et al. (2013) hurricane nature run (HNR) simulated a 13-day life cycle of a rapidly intensifying TC in the North Atlantic. The HNR was generated using the WRF model and nudged toward the ECMWF T511 global nature run (Reale et al. 2007; Masutani et al. 2009) to ensure a similar TC track in both the global and regional nature runs, while also maintaining a more realistic TC intensity and structure in the regional nature run. The model was run with four telescoping domains with a horizontal grid spacing of 27 km (outermost

TABLE 1. Characteristics of the TROPICS channels.

Channel	Central frequency (GHz)	Peak height (hPa)	Nadir footprint geometric mean (km)	Swath width (km)	FOVs	BT random error range (K)
1	91.656	1013	29.6	1779	81	[−3.4, 3.2]
2	114.50	950	24.1	1779	81	[−2.2, 2.3]
3	115.95	950	24.1	1779	81	[−2.4, 2.2]
4	116.65	930	24.1	1779	81	[−3.0, 2.6]
5	117.25	930	24.1	1779	81	[−2.7, 2.7]
6	117.80	250	24.1	1779	81	[−2.6, 2.9]
7	118.24	150	24.1	1779	81	[−3.5, 3.2]
8	118.58	60	24.1	1779	81	[−2.3, 2.2]
9	184.41	600	16.1	1779	81	[−2.4, 2.3]
10	186.51	650	16.1	1779	81	[−2.3, 2.1]
11	190.31	850	16.1	1779	81	[−2.3, 2.1]
12	204.8	900	15.6	1779	81	[−2.2, 2.4]

domain covering most of the tropical North Atlantic), 9, 3, and 1 km (innermost domain), respectively. The model has 61 vertical levels with the model top at 50 hPa. During the simulation, the TC reached a maximum intensity of approximately 120 kt (1 kt $\approx$ 0.51 m s^{-1}), a minimum sea level pressure (MSLP) around 920 hPa, and exhibited some secondary eyewall formation and eyewall replacement cycle signatures. This study focuses on the rapid intensification phase of the TC, which occurred from 1 to 5 August 2005. Figure 1 shows the HNR TC track, intensity, and MSLP with the time span covered in the current study indicated.

b. Simulated TROPICS radiances

The TROPICS constellation is designed to have six MicroMAS-2 CubeSats that are arranged in pairs across three orbital planes at an altitude of 550 km and an inclination of 30°. Each CubeSat will host a MW radiometer that takes advantage of seven oxygen absorption channels around 118 GHz to retrieve temperature soundings and three water vapor absorption channels around 183 GHz to obtain moisture soundings. The radiometer also uses one channel around 91 GHz that is sensitive to precipitation (scattering by cloud droplets and large ice crystals) and one channel at 205 GHz that is sensitive to cloud ice. Characteristics of the TROPICS channels such as central frequency, altitude at which the peak of the weighting function occurs, and nadir footprint resolution are listed in Table 1.

Brightness temperatures (BTs) for the TROPICS satellite channels were simulated from the HNR using the Community Radiative Transfer Model (CRTM) with random uncorrelated noise added (the range of the random uncorrelated noise is also listed in Table 1). Whenever the 27- and 9-km domains overlapped over the TC for a given time, the finer nest of the HNR was simply sampled spatially for the BT simulations (smoothed to the beam resolution of each channel). The simulated TROPICS BTs do not separate the V and H components of the polarization; rather, it is an averaged mean of the two components:

$$\mathrm{BT} = \cos^2(45°) \times \mathrm{BT_V} + \sin^2(45°) \times \mathrm{BT_H} = 0.5 \times (\mathrm{BT_V} + \mathrm{BT_H}).$$

Due to this mixing of polarizations, the BTs at some channels are affected more than others, as seen in the BT snapshots from channels 1, 2, 11, and 12 in Fig. 2. The deep convection and strong ice scattering near the TC center are better represented in the higher-frequency channels but not as effectively shown in the lower-frequency channels. Conversely, the deep convection in the environment of the TC is more readily apparent in the low-frequency 91-GHz channel.

The TROPICS satellites have a revisit rate of 75 min on average with a median of 40 min, made possible by the design of its three parallel orbital planes and the 30° orbit inclination. Figure 2e shows the number of revisits within a 0.25° × 0.25° grid box for the TROPICS BTs. The peak number of revisits is close to 70 for a given day. Such rapid revisits have been shown to observe the continuous evolution of TC structure and precipitation that are important for understanding TC dynamics and thermodynamics (Blackwell et al. 2018), as well as to provide high-temporal-resolution observations that could improve the analysis of TCs in NWP.

c. Simulated control observations

Simulated observations used in the control experiment include the Tropical Cyclone Vitals Database (TCVitals; NCEP 2011), Global Positioning System (GPS) radio occultation (RO) atmospheric soundings, clear-sky satellite radiances and conventional observations that were the default operational datasets assimilated in the HWRF model (Tallapragada et al. 2016). Tables 2 and 3 lists the conventional and satellite radiance data sources, respectively. This set of the control observations has been used in the previous regional OSSE studies by McNoldy et al. (2017), Annane et al. (2018) and Ryan et al. (2019). Explicit observation errors were estimated from a zero-mean Gaussian distribution with the standard deviation derived from the observation first departures (Errico et al. 2013). The control datasets were simulated from ECMWF's T511 global nature run (Reale et al. 2007) during the life cycle of the TC in the HNR. Since the HNR was nudged toward the global T511 nature run, the simulated conventional data and default clear-sky satellite radiances using the global T511 nature run presented similar synoptic conditions as in the HNR [similar discussions in section 2b in Annane et al. (2018) and section 3 in Ryan et al. (2019)]. The goal of the current TROPICS OSSE is to evaluate the new dataset's potential to improve TC prediction, which requires TROPICS data to

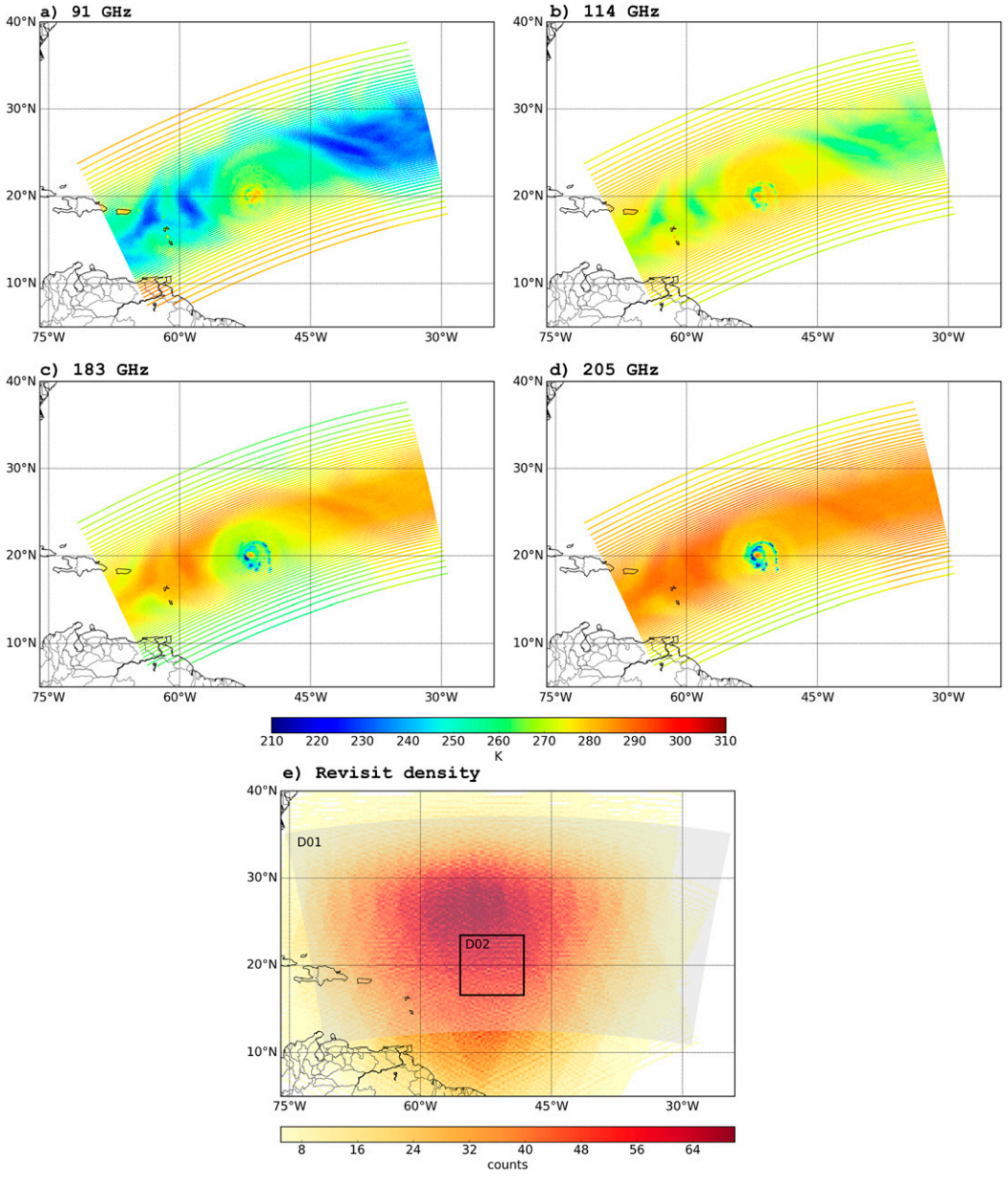

FIG. 2. (a)–(d) Simulated *CubeSat 1* brightness temperature for channels 1, 2, 11, and 12, respectively, at 0600 UTC 4 Aug 2005. (e) Number of revisits within 0.25° × 0.25° grid box on the day of 4 Aug 2005. The OSSE parent domain (D01) and inner storm-following domain (D02) is also indicated.

be simulated from a high-resolution regional nature run that has more realistic TC intensity, scale, and structure.

3. Methodology

a. Forecast model and data assimilation technique

HWRF v3.6 was used as the forecast model in a two-domain configuration with a storm-following 3-km-resolution inner nest and 9-km-resolution outer nest. This version of HWRF uses the operational model documented in Tallapragada et al. (2016), except it does not have vortex initialization/relocation and ocean coupling. The default configurations for the model physics are Ferrier microphysics, simplified Arakawa–Schubert cumulus parameterization, and the Global Forecast System (GFS) planetary boundary layer and GFDL radiation schemes, which are different from the HNR to avoid an identical twin experiment (Atlas 1997). The initial and boundary conditions of the HWRF are from a GFS model run that assimilated standard observations simulated from the global T511 nature run.

TABLE 2. Conventional data sources. Observations listed in the table are virtual (Tv) and sensible temperature (Ts), specific humidity (q), zonal (u) and meridional wind (v), and station pressure (Pstn).

Report type	PREPBUFR message type	Descriptions	Observations
120 (220)	ADPUPA	Rawinsonde	Tv, q, Pstn (u, v)
132 (232)	ADPUPA	Flight-level reconnaissance and dropsondes	Tv, q (u, v)
221	ADPUPA	Pilot balloon (pibal)	u, v
133 (233)	AIRCAR	Meteorological Data Collection and Reporting System (MDCRS) Aircraft Communications, Addressing, and Reporting System (ACARS) aircraft	Ts, q (u, v)
130 (230)	AIRCFT	Aircraft report (AIREP) and pilot report (PIREP) aircraft	Ts (u, v)
131 (231)	AIRCFT	Aircraft Meteorological Data Relay (AMDAR)	Ts (u, v)
180 (280)	SFCSHP	Surface marine reports	Tv, q, Pstn (u, v)
182 (282)	SFCSHP	Splash-level drop over ocean	Tv, q, Pstn (u, v)
181	ADPSFC	Surface land (SYNOP, METAR) reports	Tv, q, Pstn
223	PROFLR	NOAA Profiler Network	u, v
289	WDSATR	WindSat scatterometer data	u, v
290	ASCATW	Advanced Scatterometer (ASCAT) winds over ocean	u, v
224	VADWND	NEXRAD VAD winds	u, v

The serial ensemble Kalman filter (EnKF, Whitaker and Hamill 2002) is employed in this study with a 30-member ensemble. The DA is only carried out in the parent domain that covers most of the North Atlantic Ocean (Fig. 2e). Specific tuning has been done for the OSSE DA system (Bucci 2020), which includes using a posterior inflation factor of 0.9, horizontal localization length scale at 600 km, and vertical localization at one scale length (in units of ln$p$, where p is pressure in centibars).

b. Experiment design

Table 4 contains a description of the TROPICS radiance data denial experiments that are included in this study. The first set of experiments (''w/o Rad DefStateVar'') focuses on evaluating the TROPICS impact while updating the same default state variables (SVs) in the EnKF as in the operational system (Biswas et al. 2017). These SVs included zonal wind (u), meridional wind (v), temperature (T), specific humidity (q), total condensate (CWM), and hydrostatic pressure (p_d). No satellite radiances other than those from TROPICS were assimilated in the ''TROPICS'' experiments, which helps to infer the potential upper bound of the TROPICS impact.

The second set of experiments without the assimilation of default radiances (''w/o Rad'') explores the effect of updating additional cloud- and precipitation-related microphysics SVs and two more dynamical SVs with the EnKF. In the ''w/o Rad'' experiments, fraction of ice (F_ICE), fraction of rain (F_RAIN), and riming rate value (F_RIMEF) were added as SVs, based on the procedure described in Wu et al. (2019) for assimilating all-sky MW radiances when using the Ferrier-Aligo microphysics scheme (Aligo et al. 2014) in HWRF. In addition to the microphysical variables, the model layer interface pressure (PINT) and the vertical velocity variable (DWDT) [defined in the form of 1 + (dwdt)/g, where dwdt is the total derivative of vertical velocity, g is the gravity] were added. In HWRF, by default, the model is initiated with zero vertical velocity and a uniform base value of DWDT (Tallapragada et al. 2016). The inclusion of the vertical velocity variable (DWDT) will help initialize the HWRF with nonzero vertical velocity accelerations from the analysis and hence accelerate the vertical

TABLE 3. Default satellite radiance data sources. The platform names that are given as acronyms in the table include Defense Meteorological Satellite Program (DMSP), Meteosat Second Generation (MSG), and *Suomi National Polar-Orbiting Partnership* (*Suomi NPP*).

Instrument	Acronym definition	Platform(s)
AIRS	Atmospheric Infrared Sounder	*Aqua*
AMSU-A	Advanced Microwave Sounding Unit-A	*Aqua*; *MetOp-A*; *NOAA-15*, *-18*, *-19*
ATMS	Advanced Technology Microwave Sounder	*Suomi NPP*
CrIS	Cross-Track Infrared Sounder	*Suomi NPP*
GOES Sounder	Geostationary Operational Environmental Satellite	*GOES-13*
HIRS-3	High-Resolution Infrared Radiation Sounder-3	*NOAA-17*
HIRS-4	High-Resolution Infrared Radiation Sounder-4	*MetOp-A*; *NOAA-18*, *-19*
IASI	Infrared Atmospheric Sounding Interferometer	*MetOp-A*
MHS	Microwave Humidity Sounder	*MetOp-A*; *NOAA-18*, *-19*
SSMI/S	Special Sensor Microwave Imager/Sounder	DMSP *F16*
SEVIRI	Spinning Enhanced Visible and Infrared Imager	MSG

TABLE 4. Description of the experiments.

	Expt name	Assimilated datasets	Updated state variables
Expt set I	CNTL w/o Rad DefStateVar	Conventional data only	Zonal wind (u), meridional wind (v), temperature (T), specific humidity (q), total condensate (CWM), and hydrostatic pressure (p_d)
	TROPICS w/o Rad DefStateVar	Conventional data and TROPICS radiances	
Expt set II	CNTL w/o Rad	Conventional data only	Zonal wind (u), meridional wind (v), temperature (T), specific humidity (q), total condensate (CWM), and hydrostatic pressure (p_d), model-layer interface pressure (PINT), vertical velocity variable (DWDT), fraction of ice (F_ICE), fraction of rain (F_RAIN), and riming rate value (F_RIMEF)
	TROPICS w/o Rad	Conventional data and TROPICS radiances	
Expt set III	CNTL w/Rad	Conventional data and default radiances	
	TROPICS w/Rad	Conventional data, default radiances, and TROPICS radiances	

velocity growth in the model (Janjić et al. 2001; Janjić 2003), which otherwise results in a lag of the development of the TC secondary circulation, as it may take half an hour for the vertical velocity to grow in the model to represent a realistic TC circulation (Tallapragada et al. 2016). Note that DWDT and PINT state variables are routinely used in the EnKF in previous TC data impact studies (Christophersen et al. 2017, 2018).

The third set of experiments (''w/Rad'') assesses the impact of TROPICS data with satellite radiances from other platforms assimilated. The second and the third sets of these experiments both include the additional SVs described above.

For each experiment, HWRF was initialized from a cold start at 0000 UTC 1 August 2005 and cycled every 6 h through 0000 UTC 5 August 2005. The dates and times here follow the nature run time frame, not necessarily representing the time of an actual TC. A 5-day forecast is run using the analysis from each cycle. The track and intensity forecasts from each experiment are verified against the HNR. The cold start and the first three cycles in the assimilation are not included in the verification to allow for vortex spinup and model adjustments.

4. Assimilation of TROPICS radiances

To balance the number of observations between conventional datasets (listed in Table 2) and the TROPICS radiances in a given cycle, a 150-km horizontal thinning mesh was applied to the TROPICS radiances. This also made the TROPICS radiance count comparable to the per-platform radiance count for the other default satellite datasets. Of the twelve available TROPICS channels, only eight were assimilated. Channels 7 (118.24 GHz) and 8 (118.58 GHz) were excluded because their weighting function shapes are partially cut off by the HWRF model top at 50 hPa. Channels 1 (91.655 GHz) and 12 (204.8 GHz) were excluded because their radiances were used to establish the scattering index and subsequent quality control (described in section 4b). Hence, only five temperature channels (channels 2–6) and three water vapor channels (channels 9–11) were assimilated in the ''TROPICS'' experiments. To further simplify the study, TROPICS radiances over land and the 10 outermost observations in the field of view (FOV) on both sides of each scanline were excluded during preprocessing.

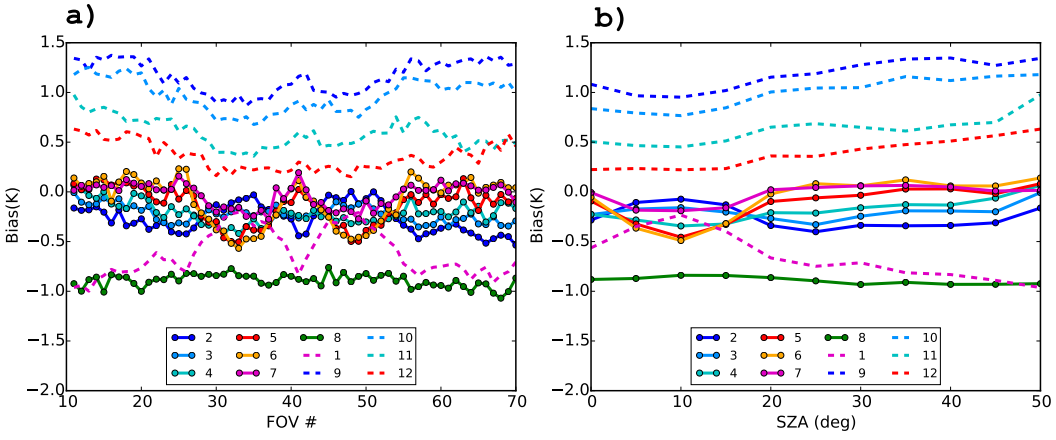

FIG. 3. First-guess departures as a function of (a) field of view (FOV) and (b) satellite zenith angle (SZA) for the evaluated unthinned TROPICS observations from the temperature channels 2–8 (solid lines), moisture channels 9–11 (dashed lines), and channels 1 and 12 (dashed lines).

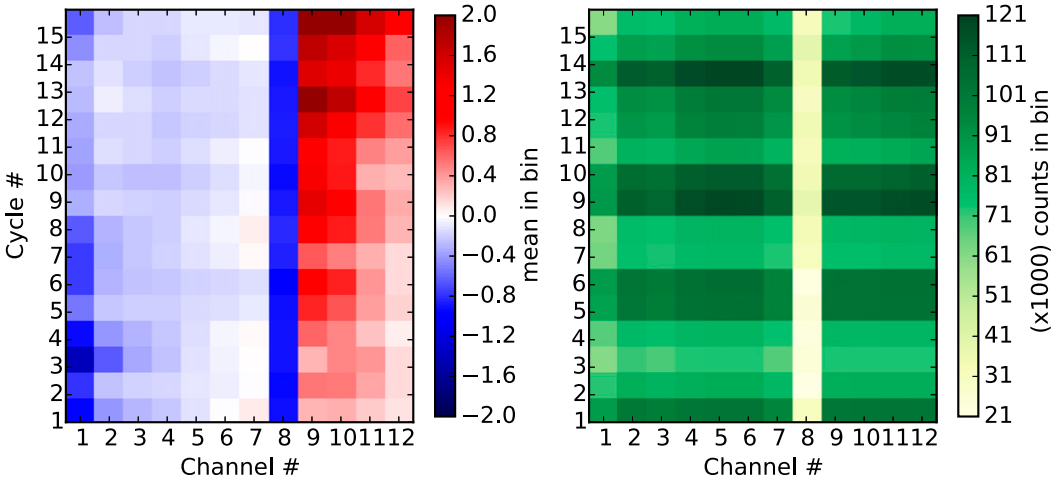

FIG. 4. Hovmöller diagram of the (left) first-guess departures and (right) number of observations for the evaluated unthinned TROPICS observations for all 12 channels.

a. *Bias correction*

Sources of biases for the simulated observations arise from the representative error between the nature run and the background or the first guess of the DA system (such as different location, shape, or intensity of the clouds or precipitation), as well as systematic model error in the forward-operator simulations. The typical satellite bias correction procedure in the GSI consists of airmass and scan-angle components in a one-step variational scheme (Derber and Wu 1998; Zhu et al. 2014). However, in the current OSSE, the non-bias-corrected first-guess departures show relatively small dependence on the scan positions or satellite zenith angle (Fig. 3), with the maximum difference less than 0.5 K. Because of this, no corrections are made for the scan-angle-dependent bias in this study. The airmass component for each channel is addressed in a simple static bias term described below. We adopt this approach mainly because the duration of TROPICS data is insufficient to perform an online estimate of bias before the first cycle (there are only three available days of data before the first cycle) and no global initial and boundary files are available beyond the 5-day period used in the study. It is also cautioned that the regional domain size might be too small to carry out online bias estimation that is typically done in the operational NWP model. For similar reasons, the first-cycle satellite biases for the default satellite observations estimated from the global GFS model run were simply adopted for all subsequent cycles.

The bias correction coefficient for each channel is estimated by taking temporal-spatial averages of the first-guess departures from all the cycles from 1 to 5 August 2005 in a test run that evaluates but does not assimilate all radiances without thinning within GSI.

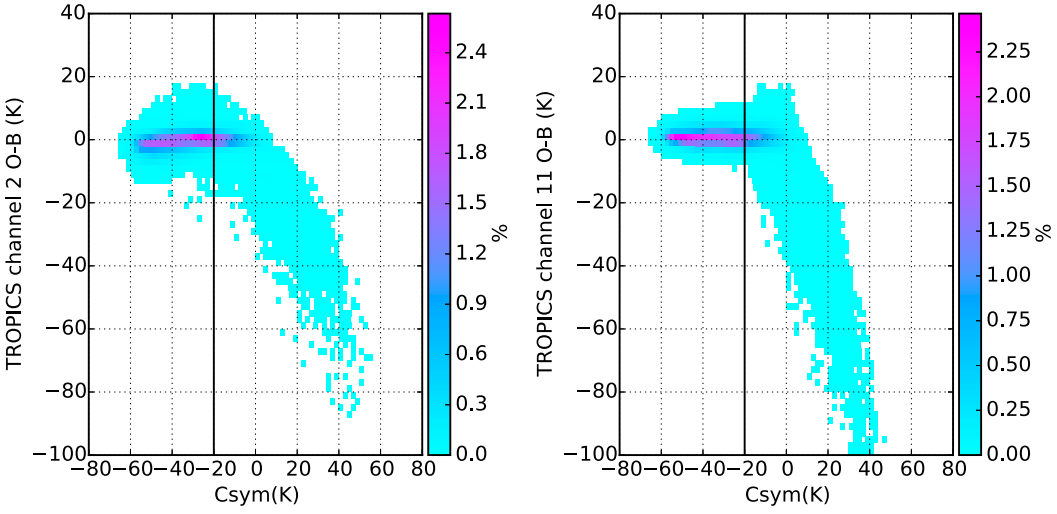

FIG. 5. Scatterplot of the symmetric cloud predictor (x axis) and first-guess departures for the TROPICS (left) channel 2 (y axis) and (right) channel 11 (y axis) using evaluated unthinned TROPICS observations from all the cycles. Color denotes the density percentage against all the data points.

TABLE 5. Parameters for the observation error model for TROPICS channels 2–6 and 9–11 (unit: K).

Channel	g_{clr}	g_{cld}	C_{clr}	C_{cld}
2	1.5	14.7	−20	5
3	0.75	13.0	−20	10
4	0.75	11.0	−20	15
5	0.75	8.2	−20	15
6	0.75	4.6	−20	15
9	2.0	15.8	−20	20
10	1.9	16.8	−20	20
11	1.8	16.9	−20	10

The bias-correction coefficients are then treated as static biases for all the cycles. The static bias as a function of the channel for all the available cycles is shown in Fig. 4a. From Fig. 4b, it is apparent there is a sufficient number of observations for each channel to support this estimation (note that more than half of channel 8's weighting function curve is above the model top). In general, the channel 1–8 biases are negative, while the channel 9–12 biases are positive. Since the variation of the biases from cycle to cycle is relatively small, the bias coefficient for each channel is estimated as the mean of the first-guess departures from all the cycles.

b. Observation errors

In all-sky radiance assimilation, the model often produces a poor estimate of clouds and precipitation as compared to the observations at a given time and location, such as different shapes, intensity, or location (Geer and Bauer 2011). The difference between the scales represented in the model versus the observations, also known as representative error, leads to non-Gaussian behavior; i.e., error increases with cloud amount. Most studies have treated this representative error in terms of observation error (Geer et al. 2014; Yang et al. 2016; Xian et al. 2019; Wu et al. 2019). Specifically, a usual approach is to apply a simple error model that takes into account the cloud amount to the radiances (Geer and Bauer 2010, 2011). For the error model used in the OSSE, two satellite channels from TROPICS are used to define the "scattering index (SI)":

$$\mathrm{SI} = \mathrm{BT}_{91} - \mathrm{BT}_{205},$$

where BT_{91} and BT_{205} are the BT of the nearest channels to 91 or 205 GHz, respectively. SI can be computed separately from the observations (SI_{obs}) or the model first guess (SI_{fg}). To account for the areas where there is cloud or precipitation in either the model first guess in the model or the observation, the symmetric cloud predictor C_{sym} is defined as

$$C_{sym} = 0.5 \times (\mathrm{SI}_{obs} + \mathrm{SI}_{fg}).$$

In theory, the larger negative values of SI indicate better agreement between the model first guess and observations in clear-sky conditions, since BTs at 91 GHz are colder than those at 205 GHz. In our study, we found that C_{sym} is nearly linearly correlated with the water vapor mixing ratio from the model first guess. Using a $C_{sym} > -20$ K threshold removes most large first-guess departures, but the threshold does not remove all the tails of the first-guess departure (Fig. 5). However, this approximate filter is sufficient to capture most of the observations that are potentially affected by cloud or precipitating-ice scattering. From this threshold, we therefore employ the following observation error model, which is similar to the error model used in Geer et al. (2014) and Lawrence et al. (2015):

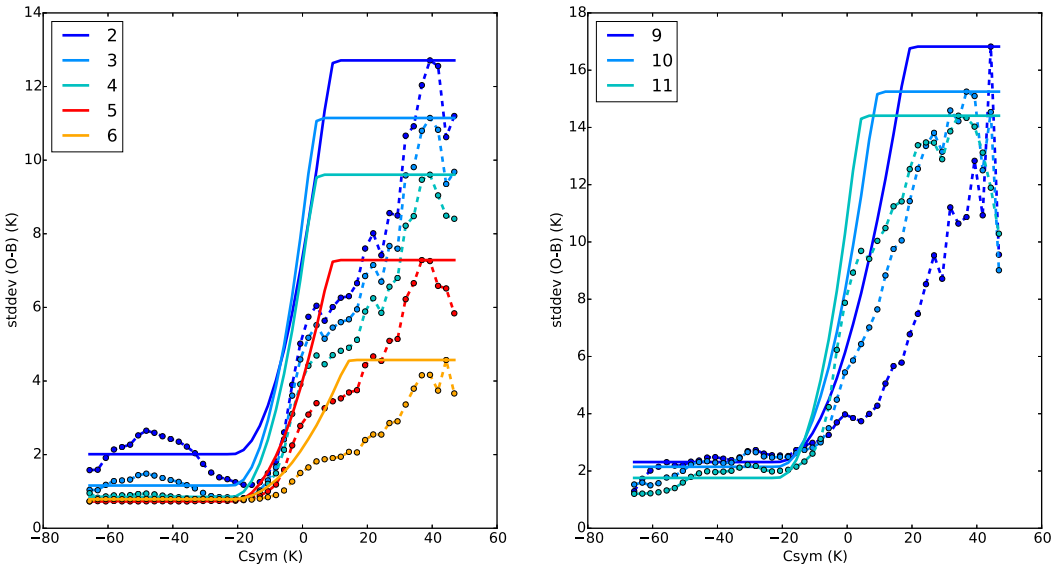

FIG. 6. Standard deviations of the observation first-guess departures as a function of the symmetric cloud predictor (dashed lines) and employed observation error models (solid lines) for TROPICS channels (left) 2–6 and (right) 9–11.

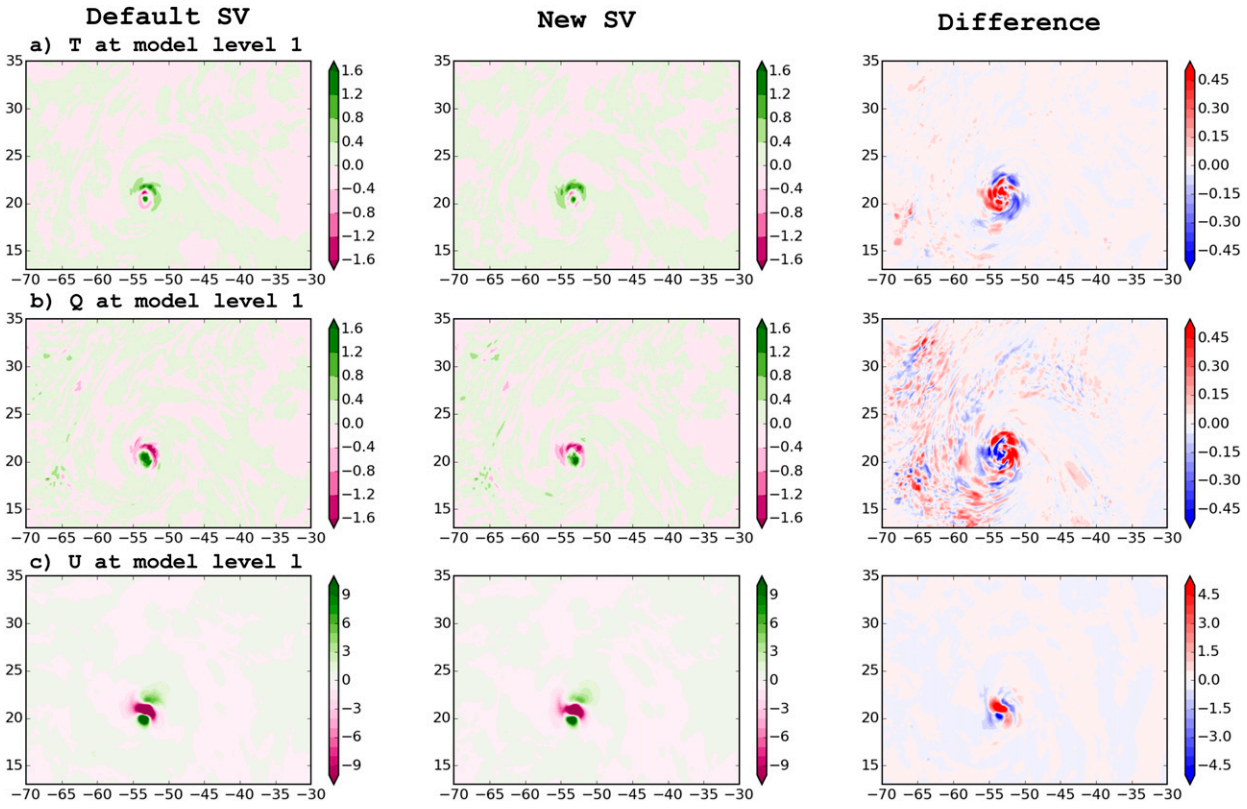

FIG. 7. Analysis increments for (a) temperature (T; K), (b) specific humidity (Q; g kg^{-1}) and (c) zonal wind speed (U; m s^{-1}) at model level one with the (left) default state variables, (center) new state variables, and (right) their differences valid at 1200 UTC 4 Aug 2005.

$$g(C_{\mathrm{SYM}}) = \begin{cases} g_{\mathrm{clr}} & \text{for} \quad C_{\mathrm{SYM}} \le C_{\mathrm{clr}} \\ g_{\mathrm{clr}} + (g_{\mathrm{cld}} - g_{\mathrm{clr}})\left(\dfrac{C_{\mathrm{SYM}} - C_{\mathrm{clr}}}{C_{\mathrm{cld}} - C_{\mathrm{clr}}}\right)^2 & \text{for} \quad C_{\mathrm{clr}} < C_{\mathrm{SYM}} < C_{\mathrm{cld}} \\ g_{\mathrm{cld}} & \text{for} \quad C_{\mathrm{SYM}} \ge C_{\mathrm{cld}} \end{cases}.$$

Here, g_{clr} and g_{cld} denote the mean (full clear-sky conditions) and maximum (full cloudy conditions) total standard deviations of the first-guess departures, and C_{clr} and C_{cld} are the parameters when the observation error increases quadratically from clear-sky conditions to cloudy conditions. Table 5 details each parameter value used for the error model. The density scatterplots of the symmetric cloud predictor and the standard deviations of the first-guess departures at the 118- and 183-GHz channels are shown in Fig. 6, with the observation errors as a function of the symmetric cloud predictor indicated as well.

5. Influence of adding new state variables in the DA

Adding new SVs has influence on various aspects of the model analyses and forecasts. First, large differences in the model analysis increments mostly close to the core of the TC are seen (Fig. 7). Together with the cycling, some differences in the near environment are seen in the humidity fields (Fig. 7b). The magnitude of the analysis increments seems to increase with TC intensity, which is also seen in the increment differences from the change of the SVs (figure not shown).

Next, the resulting analysis variation due to the addition of the new SVs is examined against the HNR. Figure 8 shows the TC 10-m wind speed and 850- and 500-hPa geopotential heights from the HNR and the TROPICS experiment with the new SVs. The TC in the OSSE presented a tighter but generally weaker vortex structure than in the HNR. We then computed the absolute analysis error between the experiment and the HNR, defining the difference of the absolute error as (i) the absolute error of the experiment with the new SVs minus (ii) the absolute error of the experiment with the default SVs, i.e., (|newSV − HNR| − |defaultSV − HNR|). Consequently, a negative difference indicates an improvement, i.e., the analysis with the new SVs is closer to the HNR than the analysis with the default SVs. Figure 8 illustrates that the resulting 10-

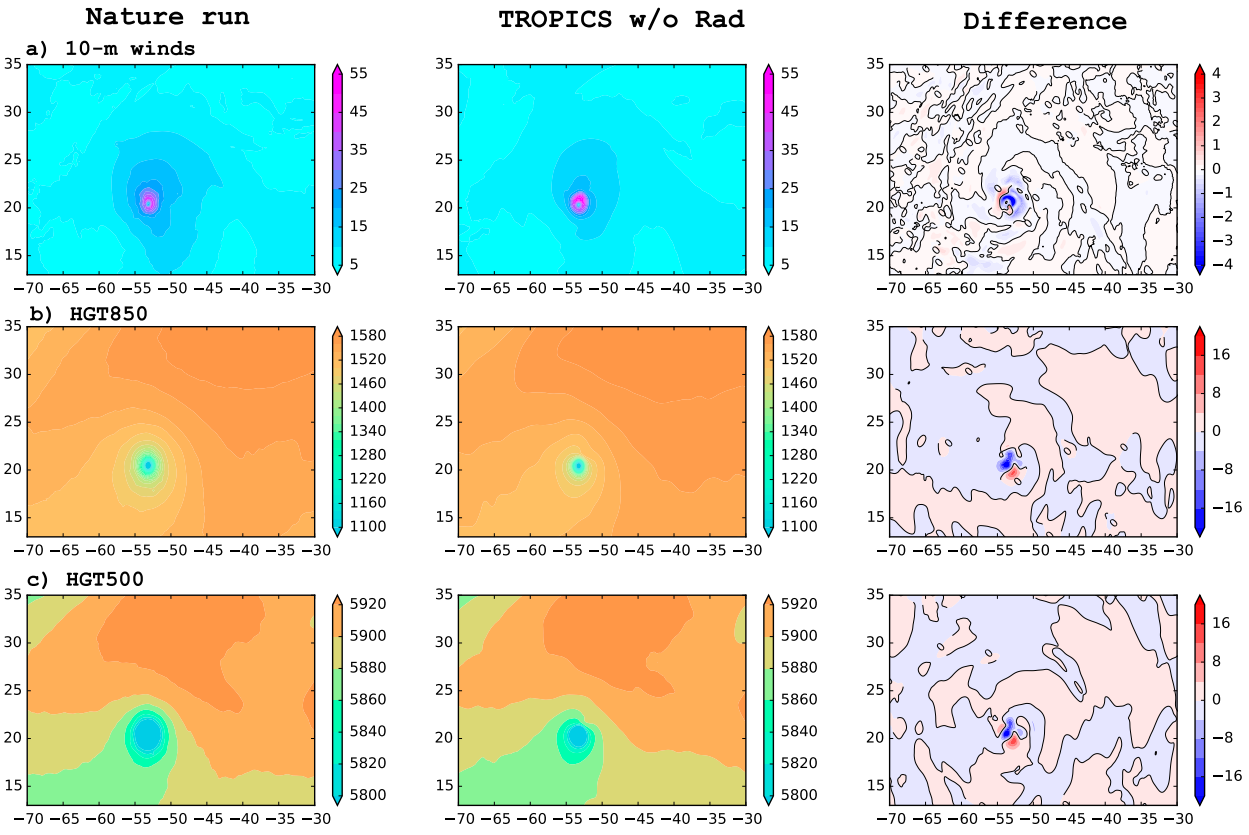

FIG. 8. (a) 10-m wind speed (m s^{-1}) and geopotential height (gpm) at (b) 850 and (c) 500 hPa from (left) the nature run and (center) the TROPICS experiment without default radiances using the new state variables valid at 1200 UTC 4 Aug 2005. (right) The impact of adding new state variables listed in Table 4 is shown, where blue colors signify the experiment with the new state variables is closer to the HNR and red colors indicate the experiment with the default state variables is closer to the HNR.

m winds and large-scale geopotential heights around the TC are most consistent with the nature run in the experiment with the new SVs. This improvement is further seen in the temperature, specific humidity and winds analyses when averaging over the HWRF domain for all the cycles (Fig. 9). Here the root-mean-square error (RMSE) difference is defined as a) the RMSE between the experiment with the new SVs and the HNR over the HWRF domain minus b) the RMSE between the experiment with the default SVs and the HNR over the HWRF domain, i.e., ($|\text{newSV} - \text{HNR}|_{\text{RMSE}} - |\text{defaultSV} - \text{HNR}|_{\text{RMSE}}$). The RMSE hereafter is computed with the biases removed, similar to Aksoy et al. (2010) and Christophersen et al. (2017). As a result, negative RMSEs signify the experiment with the new SVs in the DA presents an improvement, i.e., in the RMSE sense, the forecasts issued with the new SVs in the DA are closer to the HNR than the forecasts issued with the default SVs in the DA. At analysis time, the temperature, specific humidity, and winds in the experiment with the new SVs present smaller RMSEs at nearly all the pressure levels than those in the experiment with the default SVs. This superior performance is carried forward out to 5-day temperature forecasts at low- to midlevels, but only 2–3 days for the wind forecasts at nearly all pressure levels (Fig. 9).

Last, adding new SVs in the DA also influences the relative skill of TROPICS radiance assimilation when verifying the TC track, intensity and MSLP forecasts (Fig. 10). The relative skill is inferred from the TROPICS radiance experiments against the respective control experiments. Overall, a slight improvement in the short-range track and intensity forecasts is seen, presumably related to the short-range improvement in the wind forecasts. A consistent improvement in MSLP forecasts reveals that updating hydrometeors along with DWDT and PINT enhances the relative impact of the TROPICS radiances on TC forecasts. Based on these findings, the rest of the experiments were run using the new set of SVs.

6. TROPICS radiance impacts

Evaluation of the prior and posterior innovations of TROPICS radiances in the observation space shows some moderate improvement in the probability distribution function (PDF) distributions (Fig. 11). The assimilation shows a larger reduction in standard deviation of the PDFs in the humidity channels than the temperature channels. Some of the tails of the observations are noticeably removed. After assimilation, more data are concentrated near the zero line of the innovations, indicating some of the innovation biases are reduced.

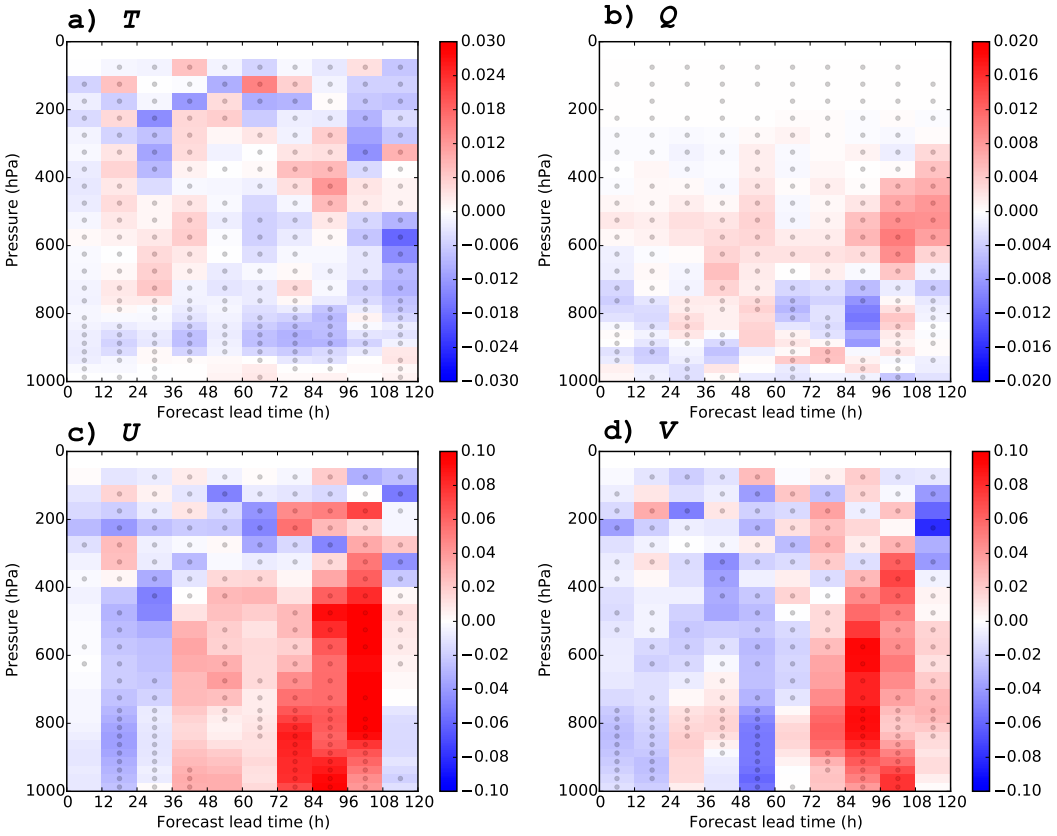

FIG. 9. Difference in root-mean-square error (RMSE) for (a) temperature (T; K), (b) specific humidity (Q; g kg^{-1}), (c) zonal wind speed (U; m s^{-1}), and (d) meridional wind speed (V; m s^{-1}) forecast fields averaged over the HWRF domain for all the cycles between the TROPICS experiment with the new state variables described in the text and the one with the default state variables verified against the HNR. The color blue signifies the TROPICS experiment with the new state variables outperforms the TROPICS experiment with the default state variables, and red indicates otherwise. The dots indicate that the experiment with the new state variables is significantly different from the experiment with the default state variables at the 95% confidence level.

The impact of assimilated TROPICS radiances on the model analysis is assessed both with and without the default radiances assimilated. A few snapshots of the model analysis from these TROPICS experiments ("TROPICS w/Rad" and "TROPICS w/o Rad," respectively) and their respective control experiments ("CNTL w/Rad" and "CNTL w/o Rad") are compared against the nature run in Figs. 12–14 . The total precipitable water (TPW) analysis (Fig. 12) highlights a dry air intrusion wrapping around the TC near environment (i.e., TPW $\leq$ 45 kg m^{-2}, Dunion 2011). The "CNTL w/o Rad" experiment shows a relatively less pronounced and moister air intrusion and a smaller, drier TC core compared to the nature run. On the other hand, the "CNTL w/Rad" experiment seems to overestimate the dryness around the TC. With the assimilation of TROPICS radiances, the under or overestimation of the dry air wrapping around the TC is improved. It is noted that the baseline radiance observations were simulated from the T511 NR only in clear-sky conditions, hence assimilating these observations presumably will largely impact the large-scale environment in the periphery of the TC. The TROPICS observations, however, were simulated from the higher-resolution HNR in all-sky conditions, which will likely contribute to the large differences we see in the TPW fields. The HNR was nudged toward the T511, which ensures the synoptic scale of the TPW fields in both NRs is close enough that we believe the differences in the TPW analysis seen here are primarily from the observations rather than a mismatch between the nature runs.

Figure 13 shows the 850-hPa temperature analysis from experiments and the respective nature run at that time. The analyses in all experiments underestimate the temperature near the core and the west side of the TC and overestimate it on the northeast side of the TC. However, the assimilation of TROPICS radiances seems to reduce the analyzed temperature when the control experiment does not include default radiances, but does the opposite when the control experiment includes the default radiances. Such contrasting impacts could be due to different information content between the default radiances from other satellite platforms and the TROPICS radiances, as

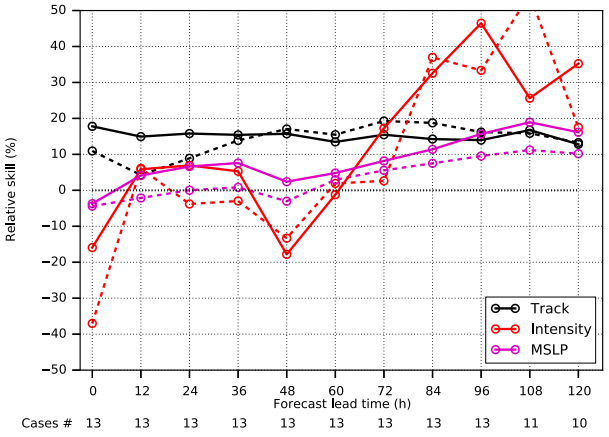

FIG. 10. Relative skill of assimilating TROPICS radiances for track, intensity, and MSLP forecasts with the default state variables (dashed lines) and the new state variables described in the text (solid lines). The relative skill is inferred from the TROPICS radiance experiments against the respective control experiments. Number of cases for each verifying forecast lead time is also indicated.

well as different bias corrections for the default radiances and TROPICS radiances. Overall, the temperature analysis from the ''TROPICS w/Rad'' experiment is closest to the nature run (Fig. 13d).

The TROPICS impact on the 500-hPa geopotential height analysis and 400–850-hPa mean steering layer is shown in Fig. 14. When default radiances are not included in the control run, the TROPICS radiances experiment generates a stronger ridge in the northern side of the TC, and a slightly stronger low- to midlevel westerly steering (Figs. 14b,c). When default radiances are present in the control run, assimilating the TROPICS radiances results in little impact on the ridge but overall brings the steering closer to the nature run in terms of the strength and direction (Figs. 14d,e).

Figure 15 shows the all-cycle, domain-averaged biases and RMSEs as a function of pressure levels for temperature, specific humidity and wind components from the TROPICS experiments and the control experiments with and without default radiances verified against the HNR. The ''TROPICS w/o Rad'' experiment exhibits the smallest RMSEs at nearly all pressure levels for all the variables. When the default radiances are not in the control experiment, the TROPICS radiances show noticeable impact on the winds and humidity analyses throughout the tropospheric column but little impact on the temperature analysis. When the default radiances are present, only small benefit of assimilating TROPICS radiances is seen in the humidity analysis, reducing the RMSE slightly in the lower troposphere. The experiments with TROPICS radiances on average show superior relative skill at nearly all pressure levels when the default radiances in the control experiment are absent. Furthermore, the largest impact on the humidity analysis is consistently seen from cycle to cycle, regardless of whether or not the default radiances are in the control experiment (figure not shown).

The TC forecast performance from the two parallel sets of TROPICS experiments is shown in Fig. 16. TROPICS data assimilation without the default radiances has a consistently positive impact (~15%) on the 5-day track forecasts, but the impact with the default radiances is mostly neutral. This could be due to the fact that the large-scale environment and steering flow influencing the TC motion is already well represented by the inclusion of the default radiances (Fig. 14). Regardless of the presence of the default radiances, the TROPICS all-sky radiances demonstrate mostly positive impacts on the intensity and MSLP forecasts. It is cautioned that the sample size here is relatively small and

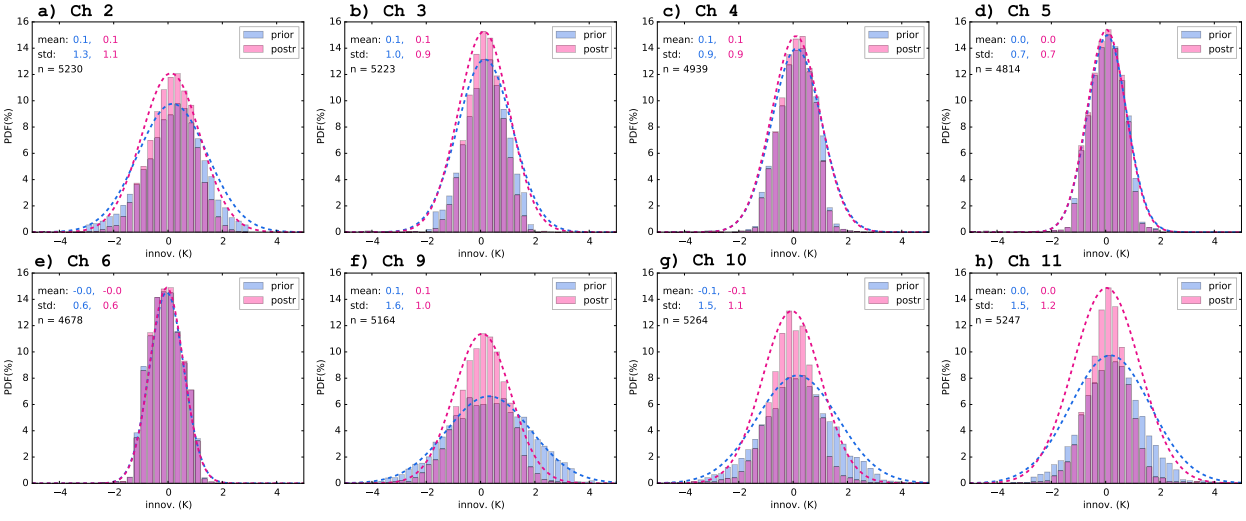

FIG. 11. Probability distribution functions (PDFs) of the prior (light blue bars) and posterior (purple bars) innovations for the TROPICS radiances for channels 2–6 and 9–11 averaged over all the cycles for the TROPICS experiment without default radiances using the new state variables described in the text. Gaussian fits (dashed lines) to the prior and posterior PDFs are also indicated.

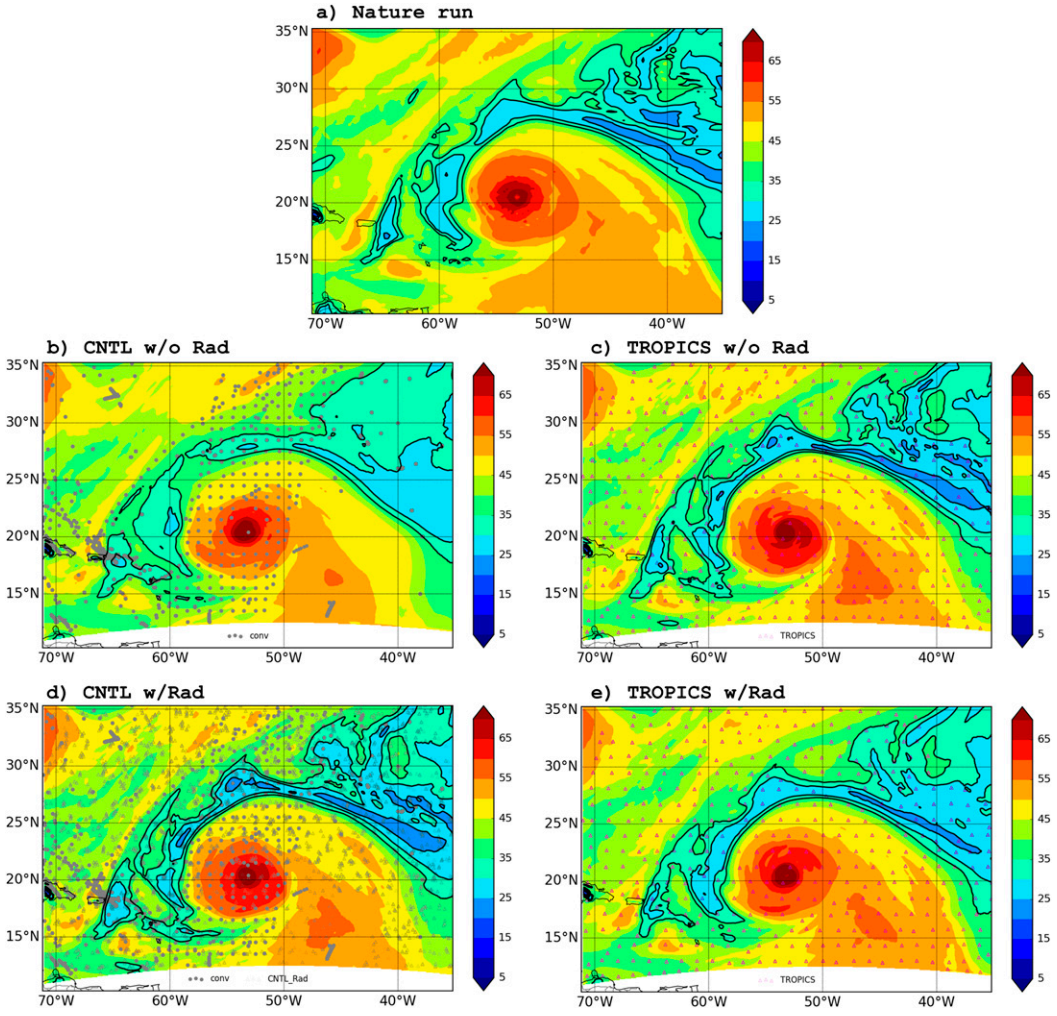

FIG. 12. Total precipitable water (kg m^{-2}) from (a) the hurricane nature run and the analysis of (b) the control experiment without default radiances, (c) the TROPICS radiance experiment with conventional data only, (d) the control experiment with default radiances, and (e) the TROPICS radiance experiment with conventional data and default radiances valid at 1200 UTC 4 Aug 2005. Values of TPW in the range 15–35 kg m^{-2} are contoured every 5 kg m^{-2}. The locations of the conventional observations are indicated with gray dots and the default radiance observation locations with gray triangles in (b)–(d). Only TROPICS observation locations are indicated with purple triangles in (c) and (e).

that this is a single case study, hence the significance of such forecast impact is difficult to assess.

The TROPICS impact with and without default radiances on the forecasts is further investigated by comparing the model forecast fields between the TROPICS experiments and the control experiments verified against the HNR. Figure 17 presents the difference in the RMSEs for the temperature, specific humdity, and wind model fields compared to the HNR averaged over the HWRF domain for all the cycles. The calculations are similar to Fig. 9 except the negative RMSEs here signify the forecasts with the assimilation of TROPICS are closer to the HNR than the forecasts without TROPICS. Note also that the magnitude of the RMSEs here is a few times larger than the one in Fig. 9. In general, TROPICS impacts on the model forecast fields are larger and more positive without the default radiances, consistent with the TC track and intensity verifications in Fig. 16. When the default radiances are not present, the improvement on temperature analysis from assimilating TROPICS is seen mostly in the 850–400-hPa layer and is maintained out to 5 days. Improvement in the specific humidity analysis at all pressure levels with the assimilation of TROPICS is carried forward from the analysis time until ~36-h lead time. Consistent positive impact of assimilating TROPICS without default radiances on winds from the surface up to 300 hPa is seen throughout the 5-day forecasts. In particular, there is a larger improvement on the zonal wind forecasts, indicating better cross track forecasts from the ''TROPICS w/o Rad'' experiment than the ''CNTL w/o

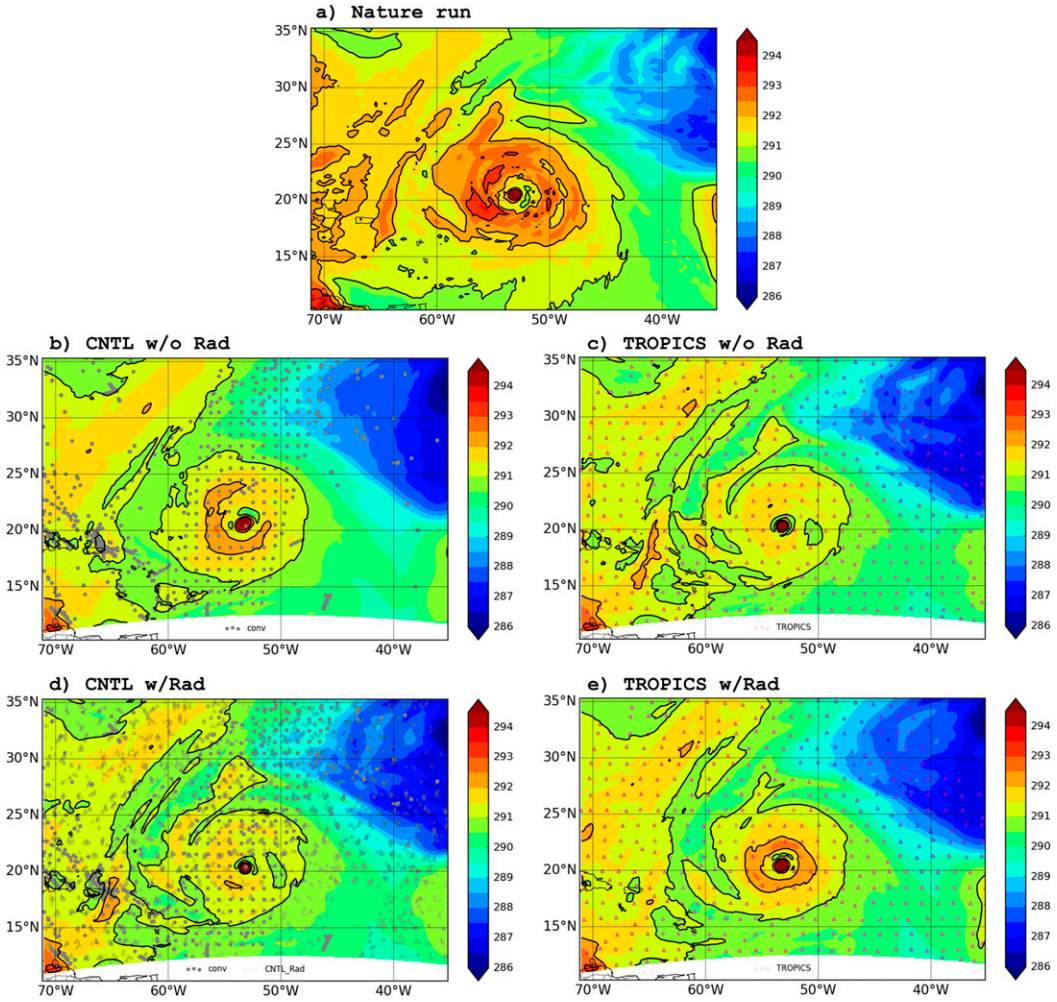

FIG. 13. As in Fig. 12, but for 850-hPa temperature (K). Values of temperature at 291, 292, and 293 K are contoured.

Rad'' experiment. When the default radiances are present, smaller reduction of the RMSEs in the model fields at all pressure levels is seen up to 36 h. Beyond that, there is some improvement in the low-level temperature and zonal wind speed forecasts. In stark contrast to the TROPICS impact without the default radiances, the assimilation of the TROPICS data with default radiances leads to a slight increase in wind forecast error beyond 48-h lead time (Figs. 17c,d right panel), particularly for the zonal wind forecasts. This behavior could be attributed to the challenges in assimilating the satellite radiances in regional models, which could increase the model errors over the domain due to ''bias correction and model top effects'' (Ryan et al. 2019). In fact, the assimilation of the default radiances seems to introduce some biases over the conventional measurements on most of the model fields at the analysis time (Fig. 15), which is particularly large for the temperature analysis. The large bias in the temperature analysis, mostly concentrated over the layer of 800–600 and 400–300 hPa, is evident throughout the 5-day forecasts (Fig. 18), though it gradually diminishes in magnitude over time. This implies that further work on better utilizing the default clear-sky radiances in the current OSSE system is warranted but beyond the scope of current study.

7. Summary and conclusions

This study examines the impact of simulated TROPICS radiance data on TC analyses and forecasts in HWRF using a regional OSSE framework. The TROPICS radiance data were simulated from the Nolan et al. (2013) hurricane nature run (HNR) using CRTM with random uncorrelated noise added. The assimilation of the TROPICS radiances was carried out using an ensemble Kalman filter with 30 ensemble members. A bias correction for each channel was estimated using the first-guess departures averaged with all the observations over the data assimilation domain for all the cycles. This estimation was mainly constrained by the limited time range covered by the global initial and boundary files that were available for use in the OSSE system. Observation errors were estimated using a symmetric cloud parameter that identifies the strongest

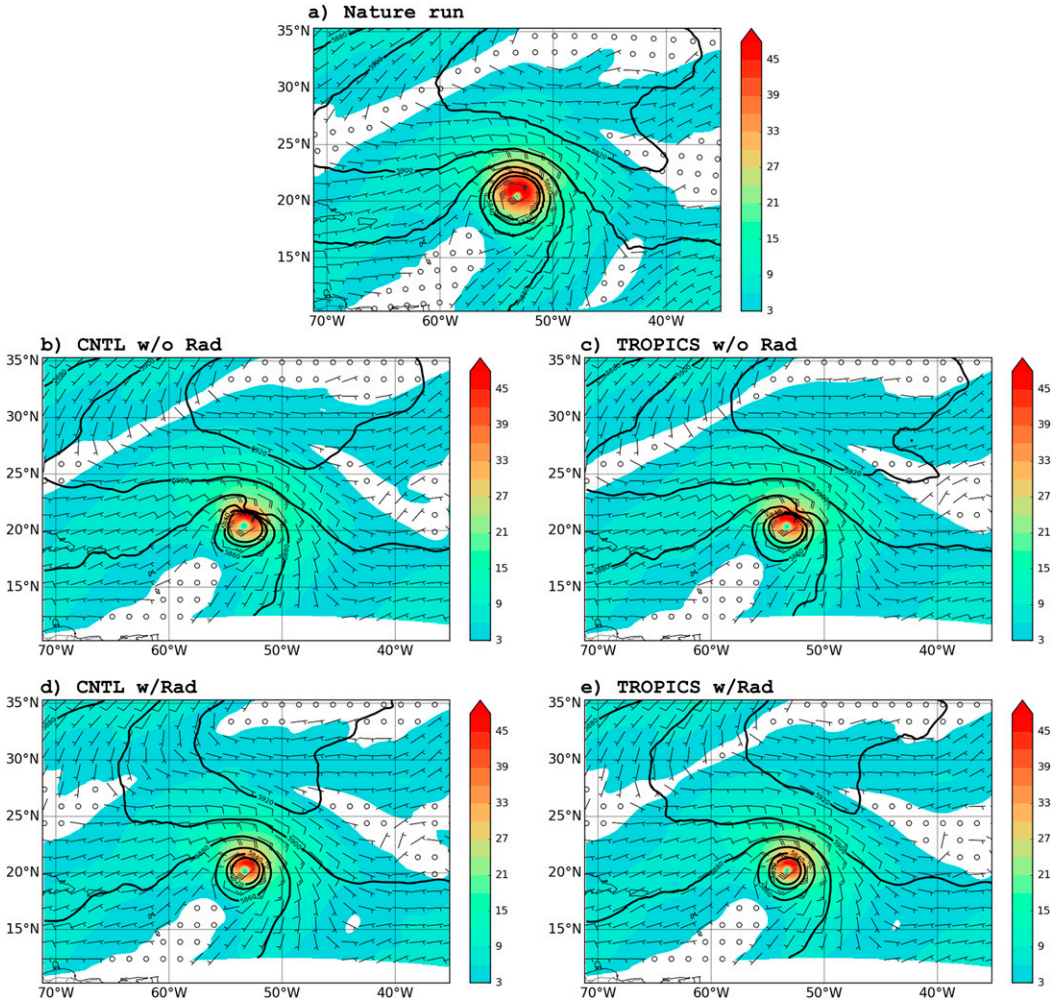

FIG. 14. 500-hPa geopotential height (gpm; contours), 400–850-hPa deep-layer-mean wind magnitude (m s^{-1}; shaded), and wind vectors (wind barbs) from (a) the HNR and the analysis of (b) the control experiment without default radiances, (c) the TROPICS radiance experiment with conventional data only, (d) the control experiment with conventional data and default radiances, and (e) TROPICS radiance experiment with conventional data and default radiances valid at 1200 UTC 4 Aug 2005.

scattering features from the radiances in two imagery channels (91 and 205 GHz) and the model first guess. Using this symmetric cloud parameter, a simple error model was then used for the assimilation of TROPICS all-sky radiances.

To better address the assimilation of TROPICS all-sky radiance data in the OSSE system, we explored adding new state variables (SVs) in the DA system and found that updating the new set of SVs in the DA improved the model analyses and forecasts. Using the new SVs appears to modify the model analysis increments around the core and the near-environment of the TC, improve the 10-m wind structure and large-scale geopotential height analysis, and present temperature, specific humidity and wind analyses that are more consistent with the HNR. The improvement on the model analysis by using the new SVs carries forward only in the short-range (up to 36 h) forecasts for the winds but lasts throughout the 5-day forecast for low-level temperature forecasts. When verifying the TC track and intensity forecasts, using the new SVs improves the relative skill of TROPICS impacts in the short-range forecasts, presumably related to the improvement only seen in the short-range wind forecasts. However, a consistent improvement on the TC MSLP forecasts is seen when using the new SVs in the DA. As such, further experiments investigating the impacts of TROPICS radiances on TC prediction used the new set of SVs.

The impact of TROPICS radiances on TC analyses and forecasts varies depending on whether the baseline satellite radiances are present in the control experiment. It is noted that the TROPICS radiances in all experiments were thinned to the extent that they are comparable to the number of the control conventional data or other satellite radiances per platform. The impact of TROPICS radiances on the analysis fields and model forecasts is generally larger when other

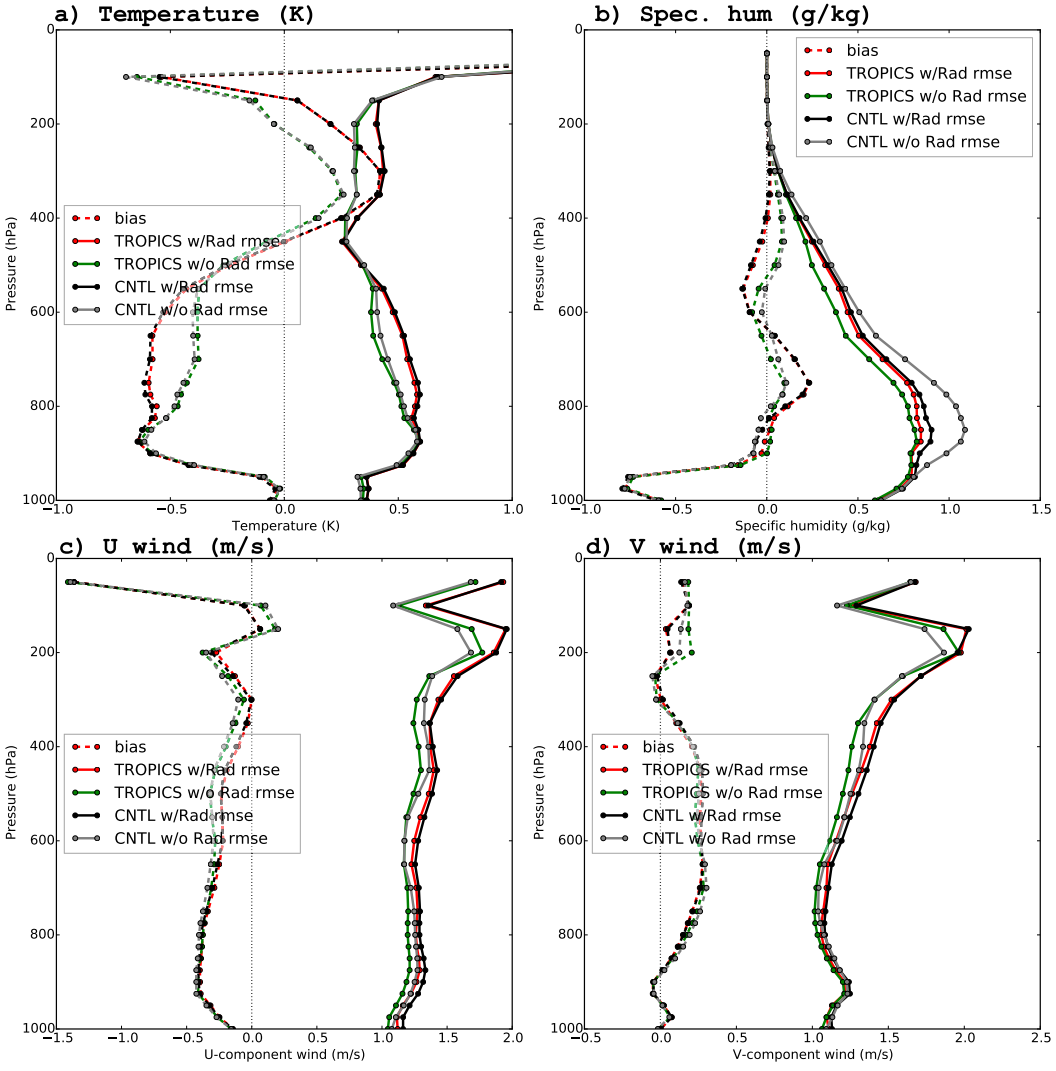

FIG. 15. All-cycle, domain-averaged bias (dashed lines) and root-mean-square error (RMSE, solid lines) of (a) temperature, (b) specific humidity, and (c) u and (d) v components of the wind analysis for the TROPICS experiments with and without default radiances, and the control experiments with and without the default radiances verified against the HNR.

satellite radiances are absent. TROPICS radiances show the largest impact on the humidity analysis, reducing the RMSEs of the humidity analysis in nearly the entire tropospheric column and consistently from cycle to cycle. Assimilating TROPICS radiances also results in consistent TC track improvement (~15%) and slight intensity improvement when other satellite radiances are absent. The assimilation of the all-sky TROPICS radiances without default radiances leads to a consistent improvement in the temperature forecasts in the 850–400-hPa layer and wind forecasts from the surface up to 300 hPa throughout the 5-day forecasts, but only up to 36-h lead time in the specific humidity forecasts at all pressure levels. When other satellite radiances are present, the TROPICS impact is small but positive for various analysis fields, presumably because the large-scale environment and steering flow may be already well depicted by the assimilation of the default radiances. This small benefit in the model fields from the TROPICS data assimilation carries forward up to 36-h lead time. We note that there are some model biases at the analysis time introduced by the assimilation of the default radiances over the conventional data, and such bias carries forward into forecasts with diminishing magnitude. Optimization to better assimilate the default satellite radiances in the current OSSE system is a topic for further study.

It is important to note that there are some limitations in the current study. It would be ideal to have the baseline datasets and TROPICS data simulated from the same nature run so the impacts of the TROPICS data assimilation can be evidently drawn from the data denial experiments. The simulated TROPICS radiance product is a mixture of horizontal and vertical polarizations, which underrepresents some of the

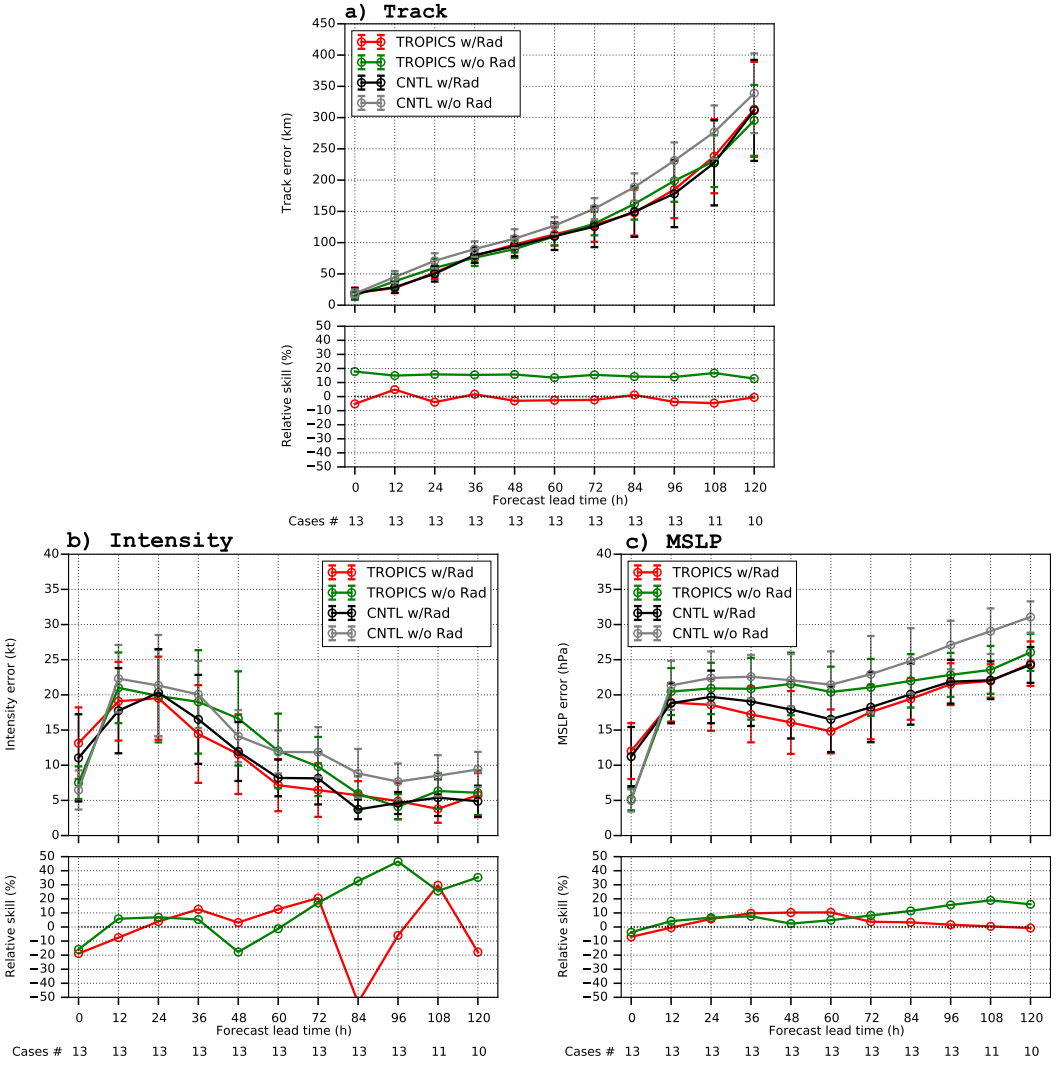

FIG. 16. All-cycle-averaged (a) track, (b) intensity, and (c) MSLP errors verified against the HNR for the control and TROPICS radiance experiments with and without default radiances. The relative skill is inferred from the TROPICS radiance experiments against the respective control experiments. The number of cases for each verifying forecast lead time is also indicated at the bottom of each panel plot.

scattering features expected from some traditional channels. The forecast model used in this study also uses parameterization schemes that are not as advanced as in the most recent, state-of-art operational HWRF model, which may further limit the TROPICS impact. We further note that more in-depth investigation could be carried out to examine the potential of the TROPICS dataset in different scenarios (e.g., assimilating temperature channels and moisture channels separately, cycling the data assimilation scheme more frequently). Additionally, more storms from additional TC nature runs should be used to address the sample size limitation in this study. Despite these limitations, the current study lays out an infrastructure to incorporate the new datasets into the operational HWRF model, which will facilitate a transition from research to operations and evaluation of the datasets once the TROPICS mission is launched.

Acknowledgments. The authors acknowledge funding support from the TROPICS Project (NA20OAR4320472), ONR Project (N0001420WX01497), and partial funding support provided through the Cooperative Agreement NA67RJ0149 between NOAA and University of Miami. H. C. acknowledges support from the NOAA Hurricane Forecast Improvement Project (HFIP) that provided the computing resources. The authors acknowledge Ralf Bennartz from Vanderbilt University for the simulation of TROPICS datasets and numerous clarifications about the datasets, TROPICS project scientist Scott Braun from NASA/GSFC for helpful discussion throughout this study. Special thanks to Sean Casey for providing the baseline simulated conventional and satellite data and Lisa Bucci for providing the nature run. The authors are also grateful for constructive suggestions from Altug Aksoy and Sim Aberson from NOAA/AOML/HRD, Will McCarty from

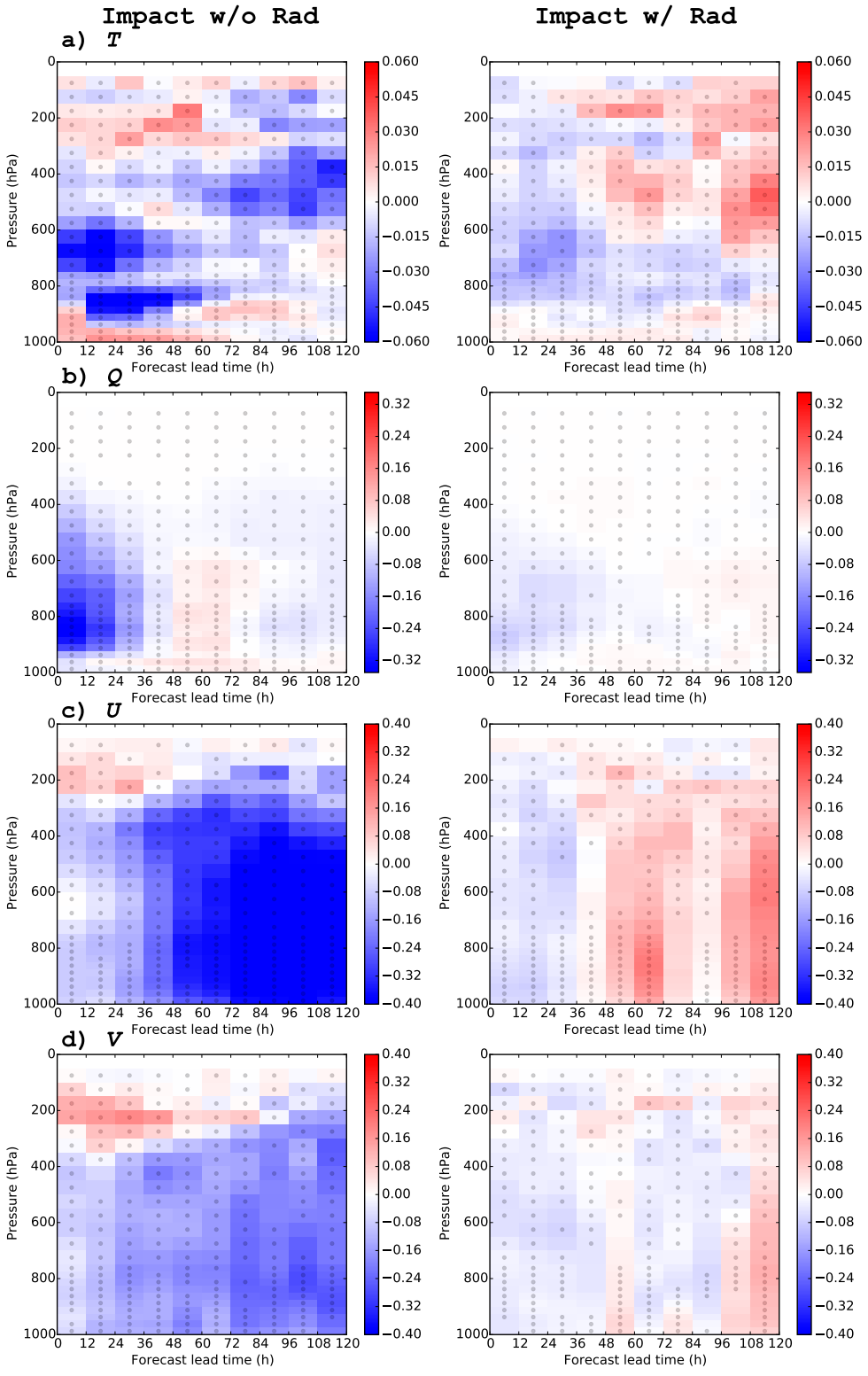

FIG. 17. As in Fig. 9, but for TROPICS impact (left) without the default radiances and (right) with the default radiances verified against the HNR. The color blue signifies the TROPICS experiment outperforms the control experiment, and red indicates the control experiment outperforms the TROPICS experiment. The dots indicate that the TROPICS experiment is significantly different from the control experiment at the 95% confidence level.

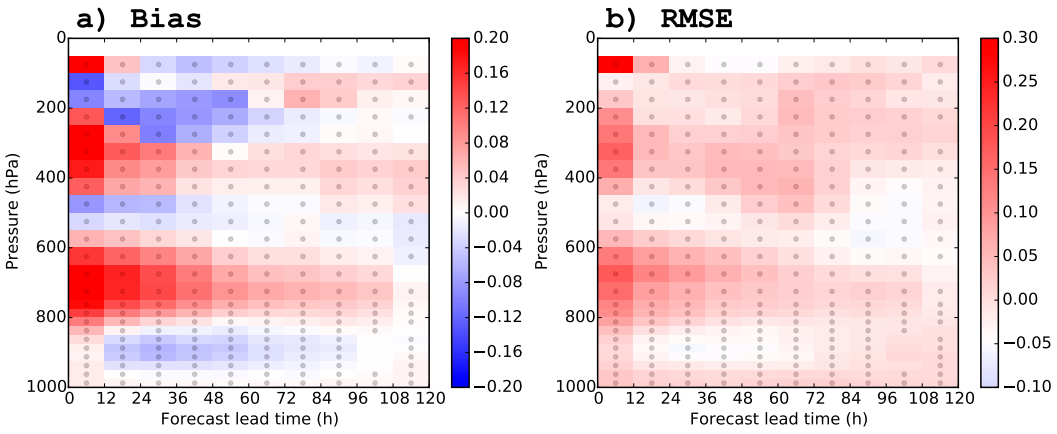

FIG. 18. Difference in the (a) absolute bias and (b) RMSE for the temperature forecasts for the TROPICS experiment with and without the default radiances verified against the HNR. The color red signifies the TROPICS experiment with the default radiances presents more biases and RMSEs than the TROPICS experiment without the default radiances. The dots indicate that the TROPICS experiment with the default radiances is significantly different from the experiment without the default radiances at the 95% confidence level.

NASA/GSFC, Jonathan Poterjoy from University of Maryland, and Henry Winterbottom from NOAA/ESPL/PSL, whose comments significantly improved the manuscript.

REFERENCES

Aksoy, A., D. C. Dowell, and C. Snyder, 2010: A multicase comparative assessment of the ensemble Kalman filter for assimilation of radar observations. Part II: Short-range ensemble forecasts. *Mon. Wea. Rev.*, **138**, 1273–1292, https://doi.org/10.1175/2009MWR3086.1.

Aligo, E., B. Ferrier, J. Carley, E. Rodgers, M. Pyle, S. J. Weiss, and I. L. Jirak, 2014: Modified microphysics for use in high-resolution NAM forecasts. *27th Conf. on Severe Local Storms*, Madison, WI, Amer. Meteor. Soc., 16A.1, https://ams.confex.com/ams/27SLS/webprogram/Paper255732.html.

Annane, B., B. McNoldy, S. M. Leidner, R. Hoffman, R. Atlas, and S. J. Majumdar, 2018: A study of the HWRF analysis and forecast impact of realistically simulated CYGNSS observations assimilated as scalar wind speeds and as VAM wind vectors. *Mon. Wea. Rev.*, **146**, 2221–2236, https://doi.org/10.1175/MWR-D-17-0240.1.

Arnold, C. P., and C. H. Dey, 1986: Observing-system simulation experiments: Past, present and future. *Bull. Amer. Meteor. Soc.*, **67**, 687–695, https://doi.org/10.1175/1520-0477(1986)067<0687:OSSEPP>2.0.CO;2.

Atlas, R., 1997: Atmospheric observations and experiments to assess their usefulness in data assimilation. *J. Meteor. Soc. Japan*, **75**, 111–130, https://doi.org/10.2151/jmsj1965.75.1B_111.

Bauer, P., E. Moreau, F. Chevallier, and U. O'Keeffe, 2006: Multiple-scattering microwave radiative transfer for data assimilation applications. *Quart. J. Roy. Meteor. Soc.*, **132**, 1259–1281, https://doi.org/10.1256/qj.05.153.

——, A. J. Geer, P. Lopez, and D. Salmond, 2010: Direct 4D-Var assimilation of all-sky radiances. Part I: Implementation. *Quart. J. Roy. Meteor. Soc.*, **136**, 1868–1885, https://doi.org/10.1002/qj.659.

Biswas, M. K., and Coauthors, 2017: Hurricane Weather Research and Forecasting (HWRF) model: 2016 scientific documentation. Developmental Testbed Center Doc., 95 pp., https://dtcenter.org/sites/default/files/community-code/hwrf/docs/scientific_documents/HWRFv3.8a_ScientificDoc.pdf.

Blackwell, W. J., 2017: Technology development for small satellite microwave atmospheric remote sensing. *Proc. IEEE Int. Microwave Symp.*, Honolulu, HI, IEEE, 222–225, http://doi.org/10.1109/MWSYM.2017.

——, and Coauthors, 2018: An overview of the TROPICS NASA Earth Venture mission. *Quart. J. Roy. Meteor. Soc.*, **144**, 16–26, https://doi.org/10.1002/qj.3290.

Bucci, L. R., 2020: Assessment of the utility of Doppler wind lidars for tropical cyclone analysis and forecasting. Ph.D. dissertation, University of Miami, 132 pp.

Christophersen, H., A. Aksoy, J. Dunion, and K. J. Sellwood, 2017: The impact of NASA Global Hawk unmanned aircraft dropwindsonde observations on tropical cyclone track, intensity, and structure: Case studies. *Mon. Wea. Rev.*, **145**, 1817–1830, https://doi.org/10.1175/MWR-D-16-0332.1.

——, ——, J. P. Dunion, and S. D. Aberson, 2018: Composite impact of Global Hawk unmanned aircraft dropwindsondes on tropical cyclone analyses and forecasts. *Mon. Wea. Rev.*, **146**, 2297–2314, https://doi.org/10.1175/MWR-D-17-0304.1.

Derber, J. C., and W. Wu, 1998: The use of TOVS cloud-cleared radiances in the NCEP SSI analysis system. *Quart. J. Roy. Meteor. Soc.*, **126**, 2287–2299, https://doi.org/10.1175/1520-0493(1998)126<2287:TUOTCC>2.0.CO;2.

Dunion, J. P., 2011: Rewriting the climatology of the tropical North Atlantic and Caribbean Sea atmosphere. *J. Climate*, **24**, 893–908, https://doi.org/10.1175/2010JCLI3496.1.

Errico, R. M., R. Yang, N. C. Privé, K. S. Tai, R. Todling, M. E. Sienkiewicz, and J. Guo, 2013: Development and validation of observing-system simulation experiments at NASA's global modeling and assimilation office. *Quart. J. Roy. Meteor. Soc.*, **139**, 1162–1178, https://doi.org/10.1002/qj.2027.

Geer, A. J., and P. Bauer, 2010: Enhanced use of all-sky microwave observations sensitive to water vapour, cloud and precipitation. ECMWF Tech. Memo. 620, 43 pp., https://www.ecmwf.int/en/

elibrary/9518-enhanced-use-all-sky-microwave-observations-sensitive-water-vapour-cloud-and.

——, and ——, 2011: Observation errors in all-sky data assimilation. *Quart. J. Roy. Meteor. Soc.*, **137**, 2024–2037, https://doi.org/10.1002/qj.830.

——, F. Baordo, N. Bormann, and S. J. English, 2014: All-sky assimilation of microwave humidity sounders. ECMWF Tech. Memo. 741, 59 pp., https://www.ecmwf.int/en/elibrary/9507-all-sky-assimilation-microwave-humidity-sounders.

——, K. Lonitz, P. Weston, M. Kazumori, K. Okamoto, Y. Zhu, and C. Schraff, 2018: All-sky satellite data assimilation at operational weather forecasting centres. *Quart. J. Roy. Meteor. Soc.*, **144**, 1191–1217, https://doi.org/10.1002/qj.3202.

Hoffman, R. N., and R. Atlas, 2016: Future observing system simulation experiments. *Bull. Amer. Meteor. Soc.*, **97**, 1601–1616, https://doi.org/10.1175/BAMS-D-15-00200.1.

Janjić, Z. I., 2003: A nonhydrostatic model based on a new approach. *Meteor. Atmos. Phys.*, **82**, 271–285, https://doi.org/10.1007/s00703-001-0587-6.

——, J. Gerrity, and S. Nickovic, 2001: An alternative approach to nonhydrostatic modeling. *Mon. Wea. Rev.*, **129**, 1164–1178, https://doi.org/10.1175/1520-0493(2001)129<1164:AAATNM>2.0.CO;2.

Kleist, D. T., and K. Ide, 2015a: An OSSE-based evaluation of hybrid variational-ensemble data assimilation for the NCEP GFS. Part I: System description and 3D-hybrid results. *Mon. Wea. Rev.*, **143**, 433–451, https://doi.org/10.1175/MWR-D-13-00351.1.

——, and ——, 2015b: An OSSE-based evaluation of hybrid variational-ensemble data assimilation for the NCEP GFS. Part II: 4DEnVar and hybrid variants. *Mon. Wea. Rev.*, **143**, 452–470, https://doi.org/10.1175/MWR-D-13-00350.1.

Lawrence, H., N. Bormann, Q. Lu, A. Geer, and S. English, 2015: An evaluation of FY-3C MWHS-2 at ECMWF. EUMETSAT/ECMWF Fellowship Programme Research Rep. 37, 26 pp., https://www.ecmwf.int/sites/default/files/elibrary/2015/10668-evaluation-fy-3c-mwhs-2-ecmwf.pdf.

Li, Z., and Coauthors, 2019: The alternative of CubeSat-based advanced infrared and microwave sounders for high impact weather forecasting. *Atmos. Oceanic Sci. Lett.*, **12**, 80–90, https://doi.org/10.1080/16742834.2019.1568816.

Masutani, M., and Coauthors, 2009: International collaborative joint OSSEs— Toward reliable and timely assessment of future observing systems. *Anthony J. Hollingworth Symp.*, Phoenix, AZ, Amer. Meteor. Soc., P1.2, http://ams.confex.com/ams/pdfpapers/149641.pdf.

McNoldy, B., B. Annane, J. Delgado, L. Bucci, R. Atlas, and S. J. Majumdar, 2017: Impact of assimilating CYGNSS data on tropical cyclone analyses and forecasts in a regional OSSE framework. *Mar. Technol. Soc. J.*, **51**, 7–15, https://doi.org/10.4031/MTSJ.51.1.1.

NCEP, 2011: Format of the tropical cyclone vital statistics records (''TCVitals''). NCEP/Environmental Modeling Center, accessed 7 June 2021, http://www.emc.ncep.noaa.gov/mmb/data_processing/tcvitals_description.htm.

Nolan, D. S., R. Atlas, K. T. Bhatia, and L. R. Bucci, 2013: Development and validation of a hurricane nature run using the joint OSSE nature run and the WRF model. *J. Adv. Model. Earth Syst.*, **5**, 382–405, https://doi.org/10.1002/jame.20031.

Reale, O., J. Terry, M. Masutani, E. Andersson, L. P. Riishojgaard, and J. C. Jusem, 2007: Preliminary evaluation of the European Centre for Medium-range Weather Forecasts' (ECMWF) nature run over the tropical Atlantic and African monsoon region. *Geophys Res. Lett.*, **34**, L22810, https://doi.org/10.1029/2007GL031640.

Ryan, K., L. Bucci, J. Delgado, R. Atlas, and S. Murillo, 2019: Impact of Gulfstream-IV dropsondes on tropical cyclone prediction in a regional OSSE system. *Mon. Wea. Rev.*, **147**, 2961–2977, https://doi.org/10.1175/MWR-D-18-0157.1.

Tallapragada, V., and Coauthors, 2016: Hurricane Weather Research and Forecasting (HWRF) Model: 2015 scientific documentation. NCAR Tech. Note NCAR/TN-522+STR, 122 pp., https://doi.org/10.5065/D6ZP44B5.

Whitaker, J. S., and T. M. Hamill, 2002: Ensemble data assimilation without perturbed observations. *Mon. Wea. Rev.*, **130**, 1913–1924, https://doi.org/10.1175/1520-0493(2002)130<1913:EDAWPO>2.0.CO;2.

Wu, T. C., M. Zupanski, L. D. Grasso, C. D. Kummerow, and S. A. Boukabara, 2019: All-sky radiance assimilation of ATMS in HWRF: A demonstration study. *Mon. Wea. Rev.*, **147**, 85–106, https://doi.org/10.1175/MWR-D-17-0337.1.

Xian, Z., K. Chen, and J. Zhu, 2019: All-sky assimilation of the MWHS-2 observations and evaluation the impacts on the analyses and forecasts of binary typhoons. *J. Geophys. Res. Atmos.*, **124**, 6359–6378, https://doi.org/10.1029/2018JD029658.

Yang, C., Z. Liu, J. Bresch, S. R. H. Rizvi, X. Y. Huang, and J. Min, 2016: AMSR2 all-sky radiance assimilation and its impact on the analysis and forecast of Hurricane Sandy with a limited-area data assimilation system. *Tellus*, **68A**, 30917, https://doi.org/10.3402/tellusa.v68.30917.

Zhu, Y., J. Derber, A. Collard, D. Dee, R. Treadon, G. Gayno, and J. A. Jung, 2014: Enhanced radiance bias correction in the National Centers for Environmental Prediction's Gridpoint Statistical Interpolation data assimilation system. *Quart. J. Roy. Meteor. Soc.*, **140**, 1479–1492, https://doi.org/10.1002/qj.2233.

——, and Coauthors, 2016: All-sky microwave radiance assimilation in NCEP's GSI analysis system. *Mon. Wea. Rev.*, **144**, 4709–4735, https://doi.org/10.1175/MWR-D-15-0445.1.